Environ Earth Sci
DOI 10.1007/s12665-015-4315-9

ORIGINAL ARTICLE

Groundwater pollution by arsenic and other toxic elements in an abandoned silver mine, Mexico

M. V. Esteller[1] · E. Domínguez-Mariani[2] · S. E. Garrido[3] · M. Avilés[3]

Received: 8 July 2014 / Accepted: 19 March 2015

Abstract This study evaluated the impact of an abandoned Ag mine on the quality of surface and groundwater. The mining site of Huautla is in south Morelos State, central Mexico. Ag–Pb–Zn and Au–Cu sulfide ores were mined in the district. The ores were characterized by the presence of Ag, galena (PbS), sphalerite (ZnS), and stromeyerite (CuAgS). Ag was the metal of greater interest. Other metals included Cu, Pb, Zn, and Au. Mining activities stopped in the early 1990s when the market price of Ag decreased; the abandoned mines then were flooded by rising groundwater levels. Because of the urgent demand for water by the inhabitants in the area, this water has been used as drinking water and as waterholes for livestock. Water sampling points included abandoned mines (América, Pajáro, Santiago, Tlachichilpa, and San Francisco), dams, and dug wells. The greatest concentrations of As and other toxic chemical elements (Fe, Mn, Pb, Cd, F) were detected in groundwater samples from flooded mines. The presence of these elements was related to the rock–water interaction process. The oxidation of sulfides appears to be the cause of increased metal concentrations in groundwater samples from flooded mine. Other possible water–rock interaction processes that can control the presence of arsenic in groundwater were the adsorption of arsenic in iron oxyhydroxides, the adsorption in carbonates, and/or coprecipitation with calcite. In the case of the San Francisco and América mines, the oxidation conditions, low correlation of As with SO_4^{2-} and Fe^{2+}, and concentrations of silica indicate that the presence of As in the groundwater could be due also to competition for adsorption sites.

Keywords Aquifer · Pollution · Arsenic · Water quality · Drinking water

Introduction

The numerous cases of pollution of groundwater by arsenic and heavy metals worldwide are related to very different geological environments: metasediments with ore bodies, volcanic formations, volcano-sedimentary formations, mining zones, hydrothermal systems, tertiary and quaternary alluvial basins, etc. (Bhattacharya et al. 2002; Smedley and Kinniburgh 2002; Rodriguez et al. 2004; Vivona et al. 2007; Gemici 2008; Armienta and Segovia 2008; Buragohain et al. 2010; Iskandar and Koike 2011). This variety of situations is defined by the particular circumstances and processes that converge in each case. That is, the presence of toxic elements in each case is a consequence of the specific geochemical environment and hydrogeologic conditions.

In mining zones, the occurrence of these toxic elements in groundwater is related to both natural (Rodriguez et al. 2004; Castro-Larragoitia et al. 2013; Wurl et al. 2014) as well as anthropic pollution processes (Carrillo-Chávez et al. 2000; Lee et al. 2005; Antunes and Albuquerque 2013). The problems created by this type of pollution are

✉ M. V. Esteller
mvestellera@uaemex.mx

[1] Centro Interamericano de Recursos del Agua (CIRA), Universidad Autónoma del Estado de México, Cerro Coatepec S/N Ciudad Universitaria, 50130 Toluca, Mexico

[2] Universidad Autónoma Metropolitana (UAM)-Unidad Lerma, Avda Hidalgo Pte, 46 Estación, 52006 Lerma de Villada, Mexico

[3] Instituto Mexicano de Tecnología del Agua (IMTA) Paseo Cuauhnáhuac, 8532 Progreso, 62550 Jiutepec, Mexico

Published online: 26 March 2015

intensified in zones where groundwater is the only supply source for the population (Armienta et al. 2001; Bhattacharya et al. 2002; Bundschuh et al. 2012; Chakraborti et al. 2013). One of these cases is the Huautla mining district (state of Morelos, Mexico), which began activities in the sixteenth century (Fig. 1). These activities only involve the extraction of mineral, which is transported to other cities in the country (San Luis Potosí, Taxco) for processing (benefit), and therefore, no mining residuals (tailings) exist there. The principal mineralizations present in this district are argentiferous galena (PbS) and sphalerite (ZnS), with silver being the metal of greatest economic interest. Other metals include Cu, Pb, Au, and Zn, but to a lesser extent.

Mining activities terminated in the early 1990s after to a decrease in the market price of Ag. When these activities ended, the mineshafts were flooded by the rising groundwater level. Because of an urgent need for water, the population in the district took advantage of this situation by installing pumps to obtain water for domestic consumption and livestock (Avilés et al. 2013).

This study evaluated the presence of arsenic and other chemically dissolved elements (Fe_T, Mn_T, Pb_T, Cd_T, F) in the groundwater in this zone and included a preliminary study of the origin of dissolved arsenic in the water. The hypothesis for the origin of the arsenic was that it and other toxic elements came from a release process related to the oxidation of sulfides present in the mineralization. Nevertheless, it is important to consider other possible water–rock interaction processes that can control the presence of arsenic in groundwater, such as adsorption of arsenic in iron oxides and hydroxides, competition for adsorption sites, and precipitation (Smedley and Kinniburgh 2002; Sracek et al. 2004; Biswas et al. 2014).

Geological setting

The study zone is in the southern region of the state of Morelos, central Mexico (Fig. 1), between 18°40′–18°20′N latitude and 90°10′–90°50′W longitude, at about 900 m above sea level. The climate is hot subhumid A(w) with an average temperature of 22.3 °C and average annual precipitation of 867 mm between May and November. During the rest of the year, precipitation is scarce.

The majority of rocks identified were extrusive igneous, most of which were andesite, followed by dacite, quartz latite, and trachyte–andesite. Small intrusions also occurred (Rodríguez-Licea et al. 1962).

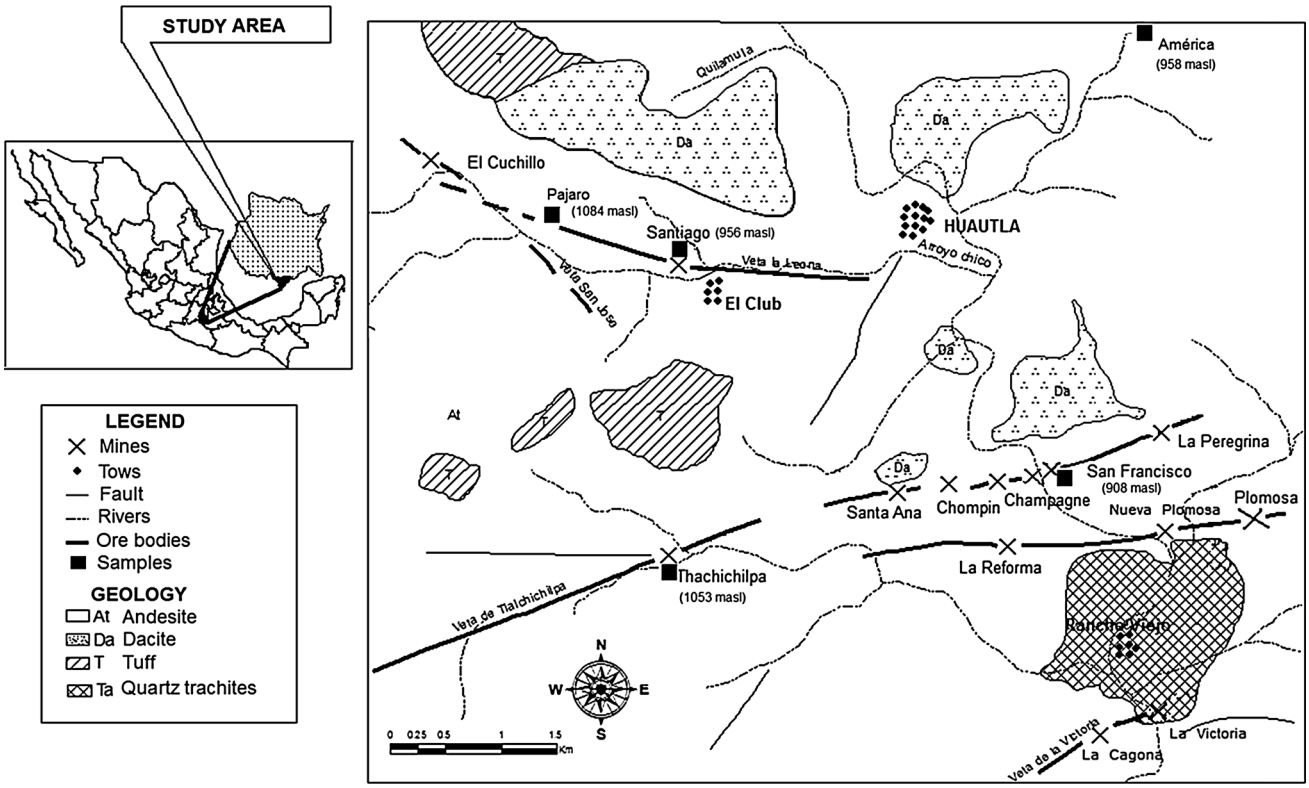

Fig. 1 Map of the location and geology of the study area. *Dark squares* show mines which are the main sampling points. The *numbers in parentheses* represent the groundwater table elevation (masl)

Ore minerals were found as filling in faults with an east–west direction, generally as tectonic breccias. The breccias showed replacement by solutions enriched with sulfide and in some areas by silica solutions. Therefore, deposits were separated by breccias in some places, where it was possible to observe the silicification of the matrix, which was composed of ferruginous clay with Fe oxides (particularly hematite) and hydroxides and cemented fragments of andesitic rock.

The most economically important minerals were argentite (Ag_2S), stromeyerite (CuAgS), and argentiferous galena (Ag–PbS). Secondary minerals were sphalerite (ZnS), chalcopyrite ($FeCuS_2$), malachite ($Cu_2CO_3(OH)_2$), azurite ($Cu_3(CO_3)_2(OH)_2$), cerussite ($PbCO_3$), and native silver. Accessory minerals included barite, pyrite, quartz, amethyst quartz, and calcite. While the studies consulted (Schulze 1959; Rodríguez-Licea et al. 1962; SECOFI 1998; SGM 2008) do not indicate the existence of arsenopyrite, its presence is not discarded since it is commonly found in deposits of this type, though in smaller quantities than arsenian pyrite ($Fe(SAs)_2$) (Armienta et al. 2001).

Table 1 shows the principal characteristics of the mines. A comparison of mineralogy and alteration processes (silicification, oxidation) shows similarities among the various mines. Table 2 presents the As, Pb, Cd, Fe, and Mn concentrations in river sediment samples throughout the study area. The highest values of these elements most likely were caused by metallic mineralization (SECOFI 1998; SGM 2008).

Materials and methods

A field survey was conducted to identify geological characteristics and sampling points. The samplings were conducted between the years 2006 and 2007, during which 16 samples were taken from five flooded mines, three samples from three dug wells and two samples from two dams. The wells and dams were north of the mining district; there were no wells or dams in the study area. The dug wells were in the alluvial deposits of the Quilamula River, whose depth was <15 m. The water was extracted with hand pumps.

The water samples were collected according to existing protocols (Boulding and Ginn 2004) and Mexican guidelines (DOF 2005). Two water samples were taken from each sampling point and filtered through a 0.45 μm disk filter, one to analyze anions (HCO_3^- SO_4^{2-}, Cl^-, NO_3^-) and the other to analyze major cations (Ca^{2+}, Mg^{2+}, Na^+, and K^+) and minor elements (As, Fe, Mn, Pb, Cd, Si, and F^-). The latter was preserved using nitric acid until reaching a pH ≤2. The samples were stored refrigerated at 4 °C until analysis.

Field determinations were conducted of pH, temperature, electrical conductivity, redox potential, and total dissolved solids with the Corning® Checkmate® Hand Held Analysis System. Field blanks and duplicates also were taken.

The following determinations were conducted in the laboratory: nitrate, sulfate, and fluoride using U-UV spectrophotometry; chloride and bicarbonate using volumetric measurements with silver nitrate and hydrochloride acid, respectively; Ca^{2+}, Mg^{2+}, Na^+, K^+, Mn^{2+}, and Si using an atomic absorption spectrophotometer (AAS); Fe, Pb and Cd, were analyzed using graphite furnace atomic absorption spectrometry; and total arsenic was determined using AAS equipped with a hydride generator. The detection limits of the elements analyzed were the following: As, 0.005 mg L^{-1}; Cd, 0.001 mg L^{-1}; Pb, 0.001 mg L^{-1}; Fe, 0.05 mg L^{-1}; Mn, 0.05 mg L^{-1}; and Si, 5 mg L^{-1}. The analyses were conducted according to procedures outlined in APHA, AWWA, and WEF (2005).

It is important to mention that other species were analyzed during the first sampling campaign, such as phosphate, ammonium, nitrite, Zn, Ag, Hg, Cu, and Cr; however, their concentrations were under the detection limit for the analytical method used, and therefore, their determinations were not included in later campaigns.

The balance error was between −6.4 and 9.4 %, and the difference between original and duplicate samples varied by ±8 %.

A database was created using the obtained results and interpreted with methods commonly used for hydrogeochemical studies, based on the basic statistics, determination of water type, relationships among parameters, correlation analysis, saturation index, and geochemical modeling. The above was carried out using AQUACHEM software (Waterloo Hydrogeologic 1999) and PHREEQC software (Parkhurst and Appelo 1999), using the database MINTEQ4.

Rock samples collected at the study site were crushed by agate mortar and pestle, and sieved <2 mm. The mineralogical composition of the rock samples was determined by X-ray diffraction (XRD) using computerized Bruker D8 Advanced XRD (equipment available from Bruker AXS Inc., Wisconsin, USA). The diffraction intensity data were scanned with a step size of 0.03° in the 2θ range from 6.5° to 110° and 88 s count time per step using Bragg–Brentano geometry. Analysis of the XRD diffraction spectra (diffractograms) was performed with DIFFRACplus software (from Bruker AXS Inc., Wisconsin, USA). These analyses were carried out in the Physics Institute at the National Autonomous University of Mexico (UNAM, Spanish acronym).

Table 1 Characteristics of the mines (SGM 2008; SECOFI 1998; Rodríguez-Licea et al. 1962)

Veins	Mines	Minerals	Secondary minerals	Matrix	Ore bodies	Enclosed rock	Grade of ore	Dimensions and reserves	AlteratiÓn
Santiago	Santiago Pájaro	Stromeyerite Argentiferous galena Sphalerite	Cerussite Pyrite Chalcopyrite Hematite	Sílica Calcedony Calcite (occasionally)	Filling of faults (tectonic breccias) Dip: subvertical Strike: NW80°	Andesite porphyry	Au = 0.5–3.0 g/t Ag = 0.85–5.0 kg/t Pb = 2.0 % Zn = 3.5 %	Length = 800 m Width = 0.5–3.0 m Shoulder = 200 m Reserves = 32,500 t	Silicification Oxidation
Tlachichilpa	Tlachichilpa	Stromeyerite Argentiferous galene Sphalerite Chalcopyrite Malachite	Chalcopyrite Hematite	Sílica Calcedony Calcite (occasionally)	Filling of faults (tectonic breccias) Dip: 45° A 61° SE Strike: NE76°	Andesite porphyry Andesite tuff	Au = Ind–1.0 g/t Ag = 0.3–2.0 kg/t Pb = 3.1–6.3 % Cu = 0.54 %	Length = 840 m Width = 0.5–4.0 m Shoulder = 220 m Reserves = 83,664 t	Silicification Oxidation Kaolinication Sericitization Chloritization
	San Francisco	Stromeyerite Galena Sphalerita Pyrite		Sílica Calcedony Calcite	Filling of faults (tectonic breccias) Dip: variable Strike: NW80°	Andesite and dacite porphyry Dike of basalt porphyry	Au = ? g/t Ag = 482–6082 g/t Zn, Cu = No data	Length = 500 m Width = 0.2 a 2.0 m Shoulder = 200 m Reserves = 25,000 t	Silicification Oxidation
América	América	Ag, Pb and Zn sulfides	Hematite	Sílica Calcedony Calcite (abundant) Malachite	Filling of faults (tectonic breccias) Dip: 45°S Strike: W60°	Andesite porphyry	Au = 0.5 g/t Ag = 482–2656 g/t Zn, Cu = No data	No data	Silicification Oxidation

Table 2 Chemical characteristics of river sediment samples in the study area ($n = 12$) (SECOFI 1998)

	As (ppm)	Pb (ppm)	Cd (ppm)	Fe (%)	Mn (ppm)
Max	148.6	1313.9	9.4	3.6	1224.2
Min	3.6	18.4	0.5	2.0	263.4
Average	12.5	54.4	0.8	2.7	561.2
SD	51.7	476.8	3.0	0.5	249.3

Results and discussion

Based on the identification of the geological characteristics of the study zone, it can be established that the volcanic materials composed a fractured aquifer where recharge was exclusively from infiltration of rainwater and discharge was from springs (two springs with low flows were identified) as well as pumping of water from the abandoned mines to meet the needs of the population in the region. It is not possible to provide more details about the hydrogeological characterization of this region in which the mining district is located, since no prior records exist, and the present study is the first of this nature to be conducted.

The piezometric levels measured in the mines (Fig. 1) indicated a likely flow direction toward the east because the highest levels were found in the Pájaro and Santiago mines and the lowest in the San Francisco mine, where the water flowed naturally from the mouth of the mine to a nearby stream.

Physicochemical parameters of water samples

Table 3 shows the principal physical–chemical characteristics of the different water samples analyzed. Samples from dug wells presented a roughly neutral pH (pH 7.16–7.67) with *Eh* values that indicated oxidation conditions. The water types were Ca–HCO_3 in the Centro and Vivero wells and Ca-SO_4 in the La Joya well (Fig. 2). The electrical conductivity was low (613–928 µS cm^{-1}). In the case of the two samples from the dams, the pH was slightly alkaline (pH 7.70–8.54) and the electrical conductivity was <460 µS cm^{-1}. The water was type Ca–HCO_3 (Fig. 2) with HCO_3^- concentrations of 234 and 109 mg L^{-1} and Ca^{2+} concentrations of 50 and 25 mg L^{-1}.

The water samples from the mines had a pH around neutral (7.16–7.67). Electrical conductivity ranged widely, between 242 and 2280 µS cm^{-1}. *Eh* values indicated oxidation conditions for all of the samples (267–466 mV). The water was type Ca-HCO_3 and only the samples from the San Francisco mine corresponded to type Na–Ca–Cl (Fig. 2) since, in this case, the dominant anion was Cl^- (899–836 mg L^{-1}). SO_4^{2-} was present to a lesser extent (288–270 mg L^{-1}), followed by HCO_3^- (174–215 mg L^{-1}). With regard to the cations, the highest concentrations were Na^+ (363–299 mg L^{-1}) and Ca^{2+} (225 to 295 mg L^{-1}). Minimal concentrations of Mg^{2+} and K^+ were detected, <12 and 8 mg L^{-1}, respectively. Si values ranged from 5.19 to 10.03 mg L^{-1}.

In the remaining mines (América, Santiago, Pájaro, and Tlachichilpa), the highest anion concentrations were bicarbonate (114–315 mg L^{-1}), with minimal concentrations for the rest of the anions: Cl^- concentrations were <55 mg L^{-1}, SO_4^{2-} <94 mg L^{-1} and NO_3^- <17 mg L^{-1}. Concentrations of major cations varied, with Ca^{2+} being the predominant cation (69–21 mg L^{-1}) and K^+ having the least concentration (2–8 mg L^{-1}). Concentrations of Si varied between 5 and 22.5 mg L^{-1}.

Groundwater from basic volcanic rocks (such as andesites and dacites, which are abundant in the study zone) was mainly bicarbonate calcic–magnesic, and the chemistry of this groundwater was related to the presence of calcite in mineralized veins and the infiltration of rainwater (Appelo and Postma 2005; Armienta et al. 2001).

The correlation coefficient matrix (Table 4) was calculated from the mine groundwater data. The Table 4 shows that the major elements had the highest coefficients. Salinity (electrical conductivity) was primarily a result of the presence of chloride, sulfate, calcium, sodium, and potassium- parameters with which there was a high correlation ($r > 0.9$). Figure 3 presents the relationships HCO_3^-–Ca^{2+} and Cl–Na^+. HCO_3^- was highly correlated with Ca^{2+}, where two sample groups must be considered (one corresponding to samples from the San Francisco mine and the other which includes the remaining samples) (Fig. 3a). This behavior also is clear in the plot of Cl–Na^+ (Fig. 3b). These differences in the water samples from the mines also can be seen in the Piper diagram (Fig. 2).

These data indicate that the water from the San Francisco mine underwent a recharge and circulation process that was different from the other mines. At this sampling point, the water flowed from the mouth of the mine to a nearby stream, which indicates a shallow groundwater table (near the soil surface), and therefore, an effect could exist from the concentration of salts from evaporation (Gutiérrez-Ojeda 2009). In addition, this point had the lowest groundwater table level of all the sampling points, and therefore, this mine could be a discharge point from this fractured aquifer and thus represent more extensive flow of groundwater.

Arsenic and toxic elements

The majority of the samples collected in the mines showed detectable concentrations of Fe, Mn, Pb, Cd, and F^-, and they all had concentrations of As with values higher than the WHO (2006) guidelines of 0.01 mg L^{-1}. In Mexico, the As limit for drinking water is 0.025 mg L^{-1} and the

Table 3 Water chemistry of samples in the Huautla mine

Samples	Date	pH	*Eh*	EC	Na^+	K^+	Mg^{2+}	Ca^{2+}	Mn	Fe
Dug wells										
Centro	05/2006	6.67	431	613	32.29	4.76	18.12	70.4	Bdl	0.12
El Vivero	05/2006	7.67	433	640	31.26	2.15	15.65	59.94	Bdl	0.10
La Joya	05/2006	6.98	354	928	33.45	52.02	24.36	120.33	**0.23**	**1.36**
Dams										
Ajuchitlan	03/2006	8.54	Nd	456	22.32	3.86	13.88	50.29	0.09	0.18
Lorenzo	03/2006	7.70	Nd	258	15.23	2.72	5.69	24.88	0.05	0.07
Mine										
America_May	05/2006	7.28	403.4	440	64.25	5.57	11.32	69.41	Bdl	0.10
America_Feb	02/2007	7.46	362.4	538	72.13	3.41	10.15	59.68	Bdl	0.05
America_Jul	07/2007	7.46	Nd	522	74.38	8.17	12.29	68.64	Bdl	0.16
Francisco_May	05/2006	7.64	423.1	2180	298.97	13.29	61.23	295.12	**0.17**	0.23
Francisco _Feb	02/2007	7.55	380.6	2168	362.65	17.97	30.21	224.69	**0.17**	0.05
Francisco _Jul	07/2007	7.35	Nd	2172	342.37	13.91	32.67	240.05	**0.26**	0.16
Pajaro_May	05/2006	7.33	466.4	356	25.12	2.03	15.11	48.71	Bdl	0.05
Pajaro_Ago	08/2006	Nd	Nd	Nd	34.31	3.44	3.06	35.49	Bdl	0.07
Pajaro_Feb	02/2007	7.63	414.2	484	31.19	3.01	14.13	42.59	Bdl	0.08
Pajaro_Jul	07/2007	7.67	Nd	396	32.97	2.36	17.60	49.54	Bdl	0.05
Santiago_May	05/2006	7.16	267.8	348	27.23	5.35	16.21	62.58	**1.64**	0.13
Santiago_Feb	02/2007	7.46	359.9	506	35.22	2.358	14.16	54.55	**1.56**	0.23
Santiago_Jul	07/2007	7.35	Nd	442	36.89	5.51	17.36	65.04	**1.99**	**0.38**
Tlachichilpa_May	05/2006	Nd	Nd	Nd	20.81	2.75	8.66	25.60	Bdl	0.05
Tlachichilpa-Jul	07/2007	7.52	Nd	242	11.10	3.75	7.66	29.61	Bdl	0.12
Tlachichilpa_Feb	02/2007	7.56	397.3	298	9.48	3.53	5.45	21.72	Bdl	**0.54**

Samples	F^-	Cl^-	SO_4^{2-}	NO_3^{2-}	HCO_3^{2-}	Si	Cd	Pb	As
Dug wells									
Centro	0.263	13.3	62.3	1.58	287	26.32	Bdl	Bdl	Bdl
El Vivero	0.498	14.5	57.5	1.66	291	13.98	Bdl	Bdl	Bdl
La Joya	0.720	20.7	258	Bdl	223	19.17	Bdl	Bdl	Bdl
Dams									
Ajuchitlan	0.344	10.8	50.0	2.16	234	16.26	Bdl	Bdl	Bdl
Lorenzo	0.252	6.5	14.8	3.61	109	16.75	Bdl	Bdl	Bdl
Mine									
America_May	0.603	55.2	94.0	1.45	276	6.07	0.002	Bdl	0.0190
America_Feb	0.568	50.8	88.2	1.13	223	12.34	0.002	Bdl	**0.029**
America_Jul	0.735	52.9	89.7	Bdl	231	8.36	0.002	**0.014**	**0.044**
Francisco_May	1.020	**899**	188.4	Bdl	215	5.19	**0.016**	**0.066**	**0.010**
Francisco _Feb	1.041	**836**	273.0	Bdl	174	10.03	0.004	**0.023**	**0.029**
Francisco _Jul	**1.510**	**857**	270.0	Bdl	178	7.38	**0.009**	**0.137**	**0.026**
Pajaro_May	0.300	2.46	5.6	17.05	289	14.46	0.001	Bdl	**0.083**
Pajaro_Ago	0.320	3.60	8.4	11.07	221	Nd	Nd	Nd	**0.098**
Pajaro_Feb	0.307	1.51	9.9	10.18	228	22.36	0.002	Bdl	**0.122**
Pajaro_Jul	0.507	4.43	11.5	6.29	248	14.31	0.001	Bdl	**0.133**
Santiago_May	0.439	7.88	43.3	0.90	315	7.73	0.002	0.046	**0.049**
Santiago_Feb	0.412	6.54	39.6	0.90	251	13.40	0.002	**0.119**	**0.088**
Santiago_Jul	0.623	6.40	43.6	0.91	265	9.33	0.002	**1.339**	**0.110**
Tlachichilpa_May	0.520	1.18	5.6	7.30	132	9.24	**0.007**	**0.267**	**0.216**

Table 3 continued

Samples	F^-	Cl^-	SO_4^{2-}	NO_3^{2-}	HCO_3^{2-}	Si	Cd	Pb	As
Tlachichilpa-Jul	0.514	0.94	7.9	3.89	119	9.43	0.001	Bdl	**0.232**
Tlachichilpa_Feb	0.334	1.51	7.2	5.36	115	16.24	0.001	Bdl	**0.261**

Concentrations in mg L^{-1} except EC (μs cm^{-1}), *Eh* (mV) and pH

Nd not determined, *Bdl* below detection limit (values in bold indicate concentration above Mexican drinking water standards)

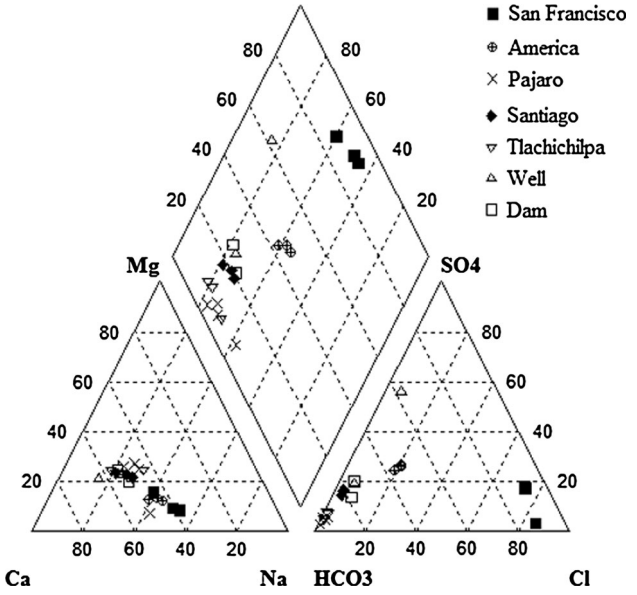

Fig. 2 Piper diagram showing the major composition of different sources of water (wells, dams, mines)

limits for Pb, Cd, Fe, Mn, and F^- are 0.01, 0.005, 0.30, 0.15, and 1.5 mg L^{-1}, respectively (DOF 2000). From the mines samples, As values between 0.019 and 0.232 mg L^{-1} were detected. Among these samples, those from the San Francisco mine had concentrations higher than the limit established by Mexican drinking water standards for Cd, Pb, Mn, and F^-; and from Santiago Mine had concentration higher than the limit for Pb, Fe, and Mn (Table 3).

Based on results from PHREEQC, which indicated an As(V) concentration ranging from 10^{-6} to 10^{-7} mol L^{-1} and As(III) under 10^{-9} mol L^{-1}, and taking into account the pH–*Eh* conditions (Table 3), arsenic was found in the form of arsenate and specifically as $HAsO_4^{2-}$, primarily in the pH range of 7.16–7.67.

In the case of water samples collected in dug wells, the presence of Cd, Pb, and As was not detected. F^- was detected, but in concentrations under 0.7 mg L^{-1}. Fe and Mn values were over the limit established by the Mexican standards in just one of the dug wells (La Joya). As, Pb, and Cd were not detected in the samples from the dams, and the concentrations of Fe, Mn, and F were <0.18, 0.09 and 0.35 mg L^{-1}, respectively.

The presence of these metals was related to mineralization. Some minerals containing As were identified in the deposits, such as galena (As concentration between 5 and 10,000 mg kg^{-1}), pyrite (As concentration between 100 and 77,000 mg kg^{-1}), and sphalerite (As concentration between 5 and 17,000 mg kg^{-1}). Mineralization was found on ferruginous clay present in breccia matrices in fractures. These clays contained Fe oxides and oxyhydroxides that could possibly be the origin of As, because these compounds can contain 200 mg kg^{-1} of As in the case of oxides and 76,000 mg kg^{-1} of As in the case of oxyhydroxides (Smedley and Kinniburgh 2002).

Some of these minerals were detected in rock samples taken in the study area. The relationship of the minerals identified in the corresponding samples using X-ray diffractogram (Fig. 4) is presented in Table 5, where the presence of pyrite (FeS), galena (PbS), and hematite (Fe_2O_3) was most notable.

Sources of arsenic

According to Smedley and Kinniburgh (2002), two factors indicate the presence of high concentrations of arsenic in groundwater. One is related to the mechanism through which As is released from the geological material that constitutes the aquifer. The other factor enables arsenic to remain dissolved in water. Since the study area is a mining region, the factor that facilitates the release of arsenic from the mineralized phase would be the oxidation of sulfurs, as indicated in previous paragraphs and demonstrated in other mining areas containing the same type of mineralization (Armienta et al. 2001; Castro-Larragoitia et al. 2013; Wurl et al. 2014, Ramos et al. 2014).

In these types of mineral deposits (with hydrothermal origins and metallic sulfurs), minerals containing arsenic can occur, including arsenopyrite and arsenian pyrite (in addition to the other sulfides), as well as oxidation products such as arsenolite (cubic form of As_2O_3) and claudetite (monoclinic form of As_2O_3) (Carrillo-Chavez et al. 2000; Smedley and Kinniburgh 2002; Armienta et al. 2001, Flakova et al. 2012). Nonetheless, the presence of these types of materials in this mining district has not been reported.

The oxidation reaction of arsenopyrite can be expressed as:

Table 4 Correlation matrix of physical–chemical parameters of groundwater samples (mines) collected (values in bold indicate significant correlation)

	pH	EC	Cl^-	HCO_3^-	SO_4^{2-}	Ca^{2+}	Mg^{2+}	Na^+	K^+	Fe	Mn	Si	As	Cd	Pb
pH	1.000	0.268	0.241	−0.394	0.069	0.222	0.329	0.213	0.122	−0.174	−0.435	0.350	0.156	0.126	−0.252
EC		1.000	**0.996**	−0.262	**0.933**	**0.984**	**0.866**	**0.987**	**0.923**	−0.097	−0.116	−0.421	−0.529	0.697	−0.081
Cl^-			1.000	−0.217	**0.930**	**0.982**	**0.859**	**0.986**	**0.930**	−0.052	−0.113	−0.456	−0.503	0.697	−0.086
HCO_3^-				1.000	−0.113	−0.071	0.058	−0.181	−0.173	−0.219	0.453	−0.102	−0.617	0.045	0.258
SO_4^{2-}					1.000	**0.912**	0.709	**0.971**	0.951	−0.116	−0.068	−0.537	−0.645	0.575	−0.047
Ca^{2+}						1.000	**0.925**	**0.961**	**0.910**	−0.042	−0.051	−0.525	−0.600	0.778	−0.019
Mg^{2+}							1.000	0.797	0.735	−0.003	−0.001	−0.448	−0.524	0.847	0.040
Na^+								1.000	**0.954**	−0.114	−0.118	−0.450	−0.566	0.633	−0.079
K^+									1.000	−0.029	−0.093	−0.543	−0.539	0.603	0.008
Fe										1.000	0.125	0.019	0.349	0.309	0.454
Mn											1.000	−0.131	−0.195	−0.052	0.802
Si												1.000	0.506	−0.514	−0.172
As													1.000	−0.416	−0.017
Cd														1.000	0.481
Pb															1.000

$$2FeAsS + 6.5O_2 + 3H_2O \leftrightarrow 2Fe^{2+} + 2SO_4^{2-} + 2HAsO_4^{2-} + 4H^+$$

The oxidation reaction of arsenian pyrite can be expressed as:

$$Fe(AsS)_2 + 6.5O_2 + 3H_2O \leftrightarrow Fe^{2+} + 2SO_4^{2-} + 2HAsO_4^{2-} + 4H^+$$

To explore this process more in-depth, the relation of arsenic with sulfates and iron was studied, given that a high correlation between these elements is not observed in the correlation matrix (Table 4) (As vs. SO_4^{3-} $r = -0.645$; As vs. Fe $r = 0.349$).

Figure 5a shows the relationship of As with SO_4^{2-} indicating a somewhat positive correlation for the samples when considering each of the mines independently; for example, $r = 0.97$ for the Pajaro mine and $r = 0.99$ for the San Francisco mine; As can be released by Fe sulfide (Smedley and Kinniburgh 2002), and these minerals were identified in samples of rocks extracted from these mines (Table 5; Fig. 4).

Figure 5a also shows two mines (San Francisco and America) with lower As concentrations than the rest of the mines. This same behavior is seen in Fig. 5b, which presents As vs. Fe, where a positive correlation ($r > 0.6$) can be seen in some of the mines, for example, Tlachichilpa, America, and Santiago. In the case of the San Francisco mine, no positive correlation between these two elements exists.

Desorption of As in Fe oxides and hydroxides is another process that could be responsible for the presence of As in the groundwater sampled from the mines, although As is desorbed if the pH increases under oxidizing conditions (Smedley and Kinniburgh 2002; Sracek et al. 2004), especially if the pH is over 8.5. If pH values reach these levels, As concentrations can increase; however, this does not appear to have occurred in the present case study because the highest pH was 7.67, and therefore, As could remain adsorbed in these mineral phases.

Another process that could explain the presence of As is the dissolution of these same Fe oxides and hydroxides under acidic conditions. While this could result in the presence of As in groundwater, these compounds of Fe oxide (as hematite) and hydroxide (as goethite and ferrihydrite) were at saturation in the mine groundwater samples and have a high potential of precipitating (Fig. 6) because the greatest precipitation occurs at an intermediate pH (Smedley and Kinniburgh 2002), as in the case of the water samples that had a pH between 7.1 and 7.6 (Fig. 7).

Arsenic mobilization

After the oxidation of sulfides takes place, other rock–water interaction mechanisms that control the presence of

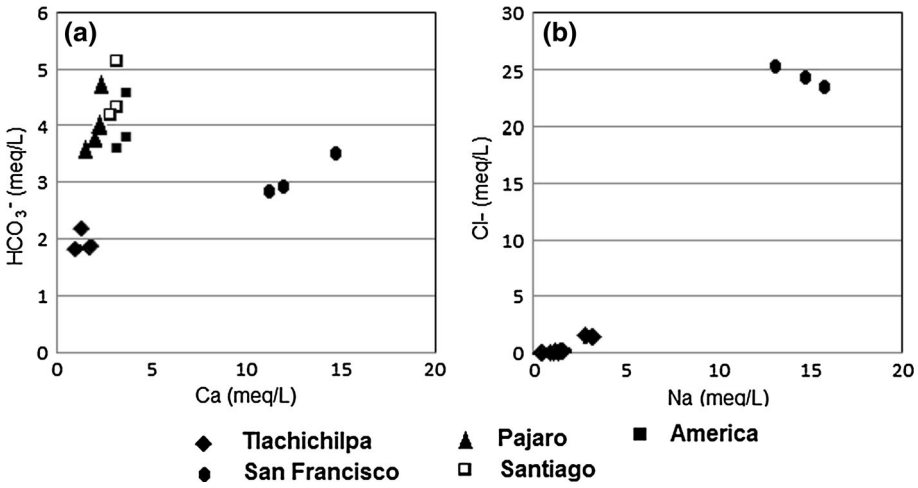

Fig. 3 *Bivariate plots* showing the relationships between **a** HCO_3^-–Ca^{2+}, and **b** Cl–Na^+

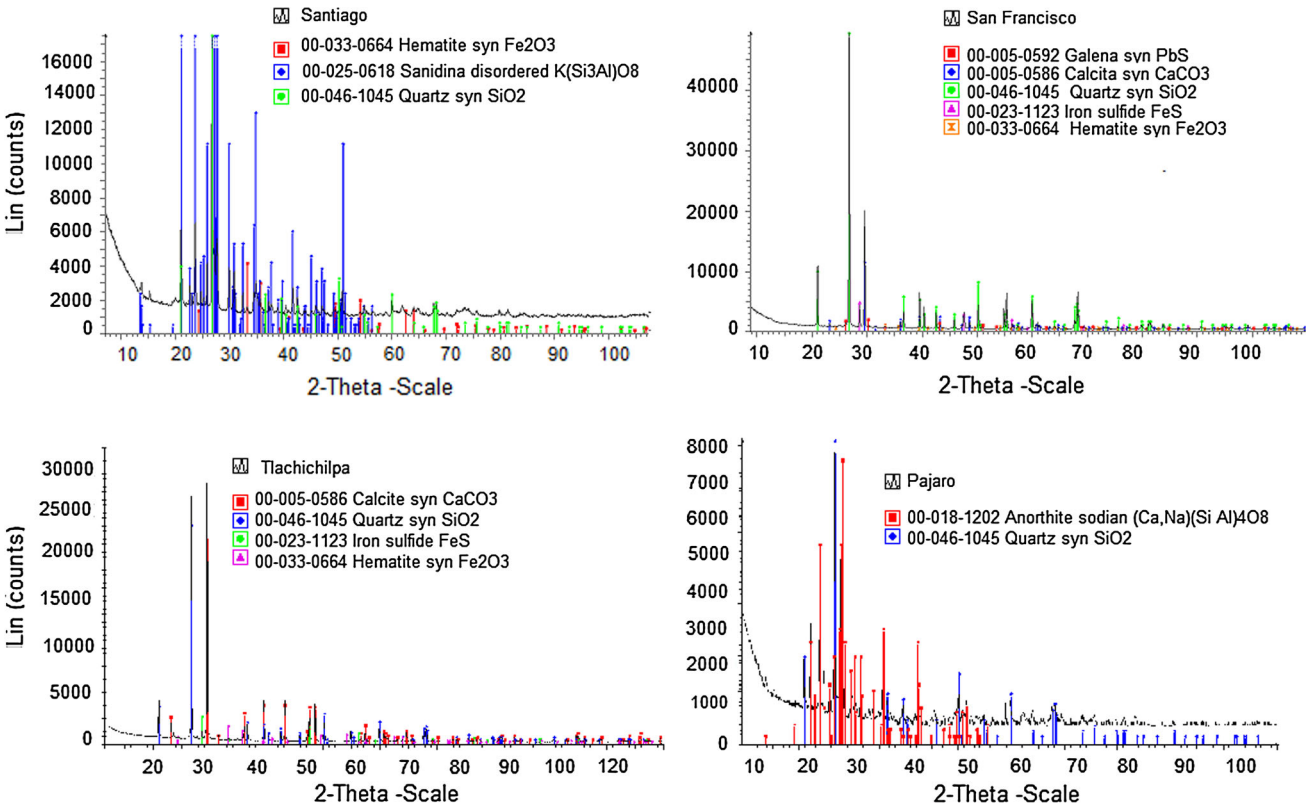

Fig. 4 X-ray powder diffraction patterns of rock samples

lower or higher concentrations of arsenic in groundwater could have occurred.

Thus, for example, low As concentrations in the San Francisco and America mines could be due to the fact that dissolved Fe tends to precipitate as iron oxides and oxy-hydroxides, or as Fe sulfates, at the same time producing an adsorption process and/or the coprecipitation of arsenic (Wilkie and Heering 1996; Flakova et al. 2012). For example,

$$Fe^{2+} + 0.25O_2 + 2.5H_2O \leftrightarrow Fe(OH)_3 + 2H^+ \text{ (ferrihydrite)}$$

$$Fe^{2+} + 2H_2O \leftrightarrow FeOOH + 3H^+ \text{(goethite)}$$

$$2Fe^{3+} + 3H_2O \leftrightarrow Fe_2O_3 + 2H^+ \text{ (hematite)}$$

As(V), in the form of arsenate, can be adsorbed by these Fe compounds (Sracek et al. 2004).

In addition, competitive adsorption of anions could occur. To study this possible behavior of As in water from

Table 5 Mineral phases identified from DRX patterns of the rock samples of the Huautla mining district

Mineral	Composition	Santiago	Tlachichilpa	San Francisco	Pajaro
Sanidine	$K(Si_3Al)O_8$	✔			
Quartz	SiO_2	✔	✔	✔	✔
Hematite	Fe_2O_3	✔	✔	✔	
Calcite	$CaCO_3$		✔	✔	
Pyrite	FeS		✔	✔	
Galena	PbS			✔	
Anorthite	$(CaNa)(SiAl)_4O_2$				✔

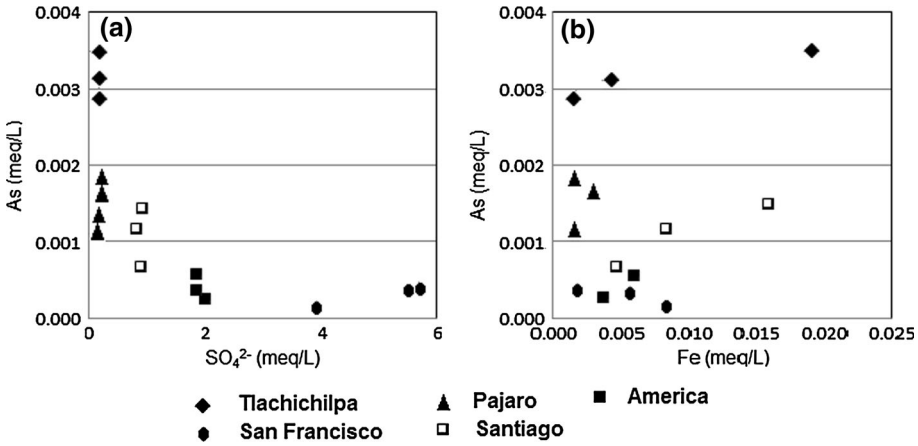

Fig. 5 *Bivariate plots* showing the relationships between **a** As-SO_4^{2-}, and **b** As–Fe

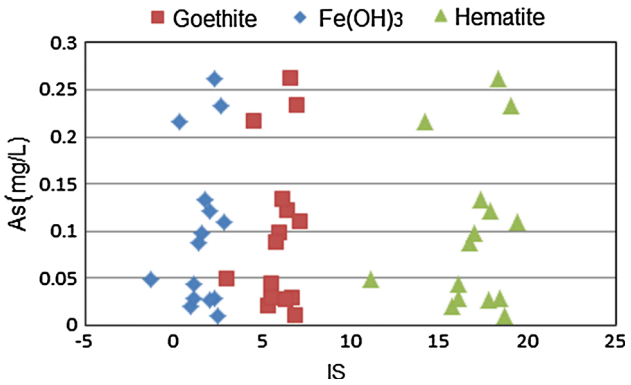

Fig. 6 *Bivariate plot* showing the relationships between As-$Fe(OH)_{3a}$ saturation index, As-goethite saturation index, and As-hematite saturation index

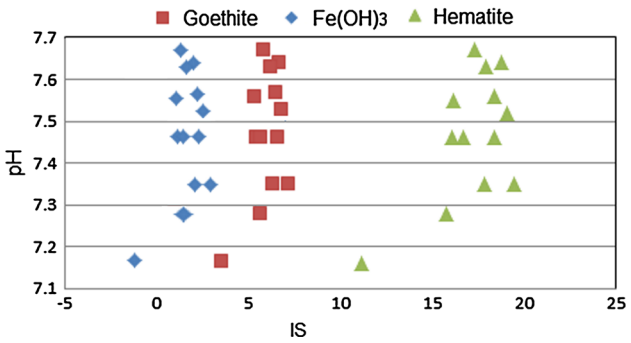

Fig. 7 *Bivariate plot* showing the relationships between pH-$Fe(OH)_{3a}$ saturation index, pH-goethite saturation index, and pH-hematite saturation index

the San Francisco and America mines, which had the highest ionic content (Table 3), relationships between As and other anions (sulfate, bicarbonate, silicate, phosphate, and molybdate) were analyzed because a competitive adsorption among anions process could have occurred in the groundwater (Sracek et al. 2004; Gao et al. 2011; Biswas et al. 2014). Figure 8a shows a negative correlation between As and HCO_3^-, indicating that the source of As could not have been adsorption competition with bicarbonate because a lower arsenic concentration was detected in water when bicarbonate was in the medium. Figure 8b shows a negative As saturation index of calcite relationship and confirms that the anion HCO_3^- does not compete for sorption sites, because more arsenic is present in the water when groundwater has a tendency to dissolve more calcite. This negative correlation could indicate other processes, given that arsenate also can be absorbed on carbonates and/or coprecipitated with calcite, and therefore, when calcite is precipitated, a decrease in the concentration of As in water is observed (Armienta et al. 2001; Winkela et al. 2013). This is particularly true for the

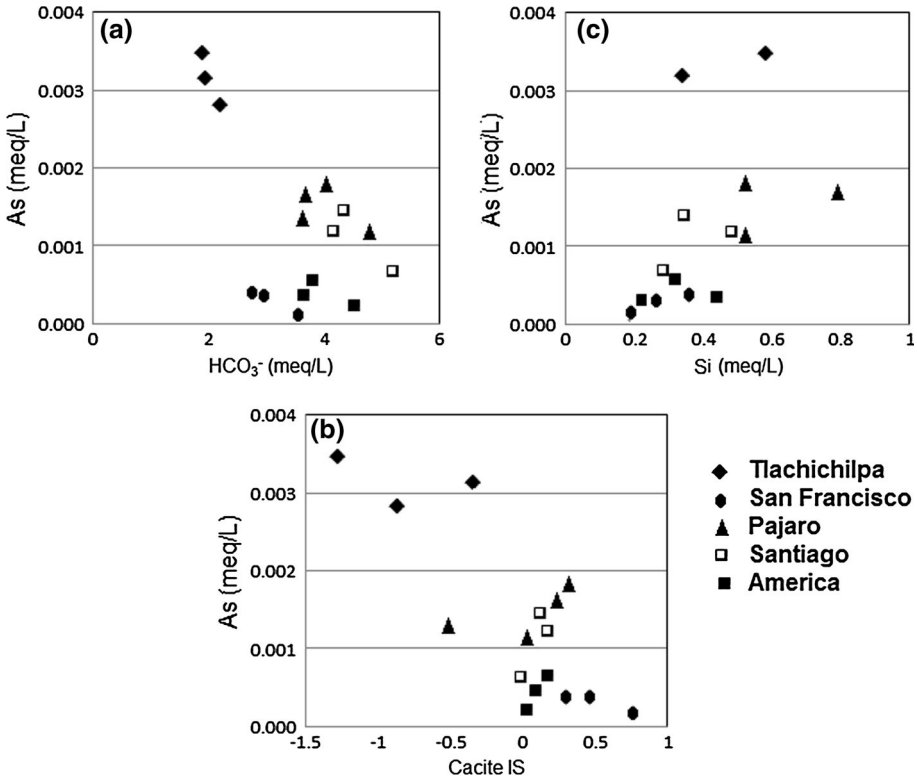

Fig. 8 *Bivariate plots* showing the relationships between **a** As-HCO_3^-, **b** As-calcite saturation index, and **c** As–Si

Table 6 Saturation index of the mine groundwater samples

	As(3)	As(5)	Maghemite	Magnetite	Mg-Ferrite	$Fe(OH)_{2.7}C_{l0.3}$	$Fe_3(OH)_8$	Jarosite-H	Jarosite-K	Jarosite-Na
America_May	9.4E−15	2.54E−07	5.76	16.85	6.24	6.07	0.49	−5.46	0.68	−1.64
America_Feb	2.9E−14	5.16E−07	5.36	16.64	6.32	5.81	0.16	−6.68	−0.63	−2.67
America_Jul	1.4E−16	5.89E−07	8.00	19.42	9.04	7.13	2.93	−2.73	3.70	1.29
Francisco_May	3.3E−17	1.34E−07	8.42	20.15	10.26	7.65	3.79	−4.07	2.77	0.75
Francisco _Feb	5.3E−15	3.81E−07	5.74	17.03	7.22	6.32	0.56	−5.91	0.92	−1.14
Francisco _Jul	1.7E−16	3.50E−07	7.42	18.66	8.55	7.23	2.17	−2.60	3.92	1.95
Pajaro_May	6.7E−17	1.11E−06	6.88	17.63	7.95	6.21	1.03	−6.10	−0.45	−2.72
Pajaro_Feb	1.5E−14	1.63E−06	6.60	18.44	8.09	5.92	1.96	−7.33	−1.15	−3.51
Pajaro_Jul	2.8E−17	1.78E−06	7.50	18.45	9.15	6.50	1.96	−6.06	0.06	−2.17
Santiago_May	1.1E−09	6.53E−07	0.81	11.85	1.23	3.38	−4.51	−13.06	−7.05	−9.72
Santiago_Feb	9.4E−14	1.17E−06	6.25	18.31	7.46	5.99	1.76	−5.95	−0.08	−2.27
Santiago_Jul	3.7E−16	1.47E−06	9.04	21.08	10.03	7.41	4.59	−1.35	4.81	2.26
Tlachichilpa-Jul	2.0E−16	3.10E−06	7.96	19.30	9.00	6.58	2.81	−4.95	1.22	−1.68
Tlachichilpa_Feb	9.6E−12	3.49E−06	4.05	14.69	2.90	4.91	−1.41	−8.21	−2.64	−5.62

Positive values indicate dissolution, negative values indicate precipitation

case of the San Francisco mine. The diagenetic precipitation of calcium arsenates ($Ca_5H_2(AsO_4)_4{\cdot}cH_2O$) could also control the mobilization of arsenic (Martínez-Villegas et al. 2013), but since the correlation between the two elements is negative (Table 4), this process is not expected to occur.

Silicate is another anion that could compete for adsorption sites. Figure 8c indicates a correlation with a positive trend between As and Si (San Francisco mine), and thus, this species could contribute to the desorption of arsenic because the concentration of arsenic in water tends to increase when there is more silica in the aqueous solution.

Table 7 Result for the modeling water–rock interaction process

	pH	pe	As	m_$HAsO_4^{-2}$	m_H_2AsO^{4-}	m_AsO_4^{-3}	m_H_3AsO_4	si_Calcite	si_Goethite	si_$Fe(OH)_3$(a)	si_Hematite
1. Sample: Francisco-Jul	7.35	4.00	3.50E−07	2.83E−07	6.73E−08	4.91E−11	4.33E−13	0.3019	7.650	1.758	17.308
2. Equilibrium and exchange with calcite	7.32	3.56	1.73E−07	1.38E−07	3.56E−08	2.17E−11	2.47E−13	0	6.845	0.957	15.697
3. Adsorption onto iron oxyhydroxides surface	7.32	3.56	1.73E−07	1.38E−07	3.56E−08	2.17E−11	2.47E−13	0	6.845	0.957	15.697
4. Final solution	7.19	11.64	1.17E−07	8.69E−08	2.98E−08	1.04E−11	2.75E−13	0	8.644	2.752	19.296

Geochemical modeling

Since various water–rock interaction processes exist that could explain why different arsenic concentrations are detected in the groundwater sampled from the mines, geochemical modeling was performed to verify which processes may be more strongly involved.

In a first step, the saturation indices of different mineral species (besides the saturation index of calcite and hematite, goethite, and ferrihydrite) were calculated, with special attention to those species that are constituted by arsenates. The possibility of precipitation of calcium arsenate ($Ca_3(AsO_4)_2$) or hydrated calcium arsenate ($Ca_3(AsO_4)_2{\cdot}cH_2O$; c = 2,4 or 8) compounds was assessed, and the data showed that this mineral species cannot be formed.

Positive values of saturation index have other mineral phases as maghemite, magnetite, Mg-Ferrite, $Fe(OH)_{2.7}Cl_{0.3}$ and $Fe_3(OH)_8$, all of which are oxides and hydroxides of Fe-, which indicate their tendency to precipitation (Table 6). Furthermore, the corresponding mineral phases of iron sulfates (Jarosite-H and Jarosite-K Jarosite-Na) tend to remain in solution.

In a second step, the processes of interaction between arsenic and iron hydroxides (Carrillo and Drever 1998), as well as calcite were modeled. The sample from San Francisco mine (sampling of July) was selected (Table 7). This modeling was carried out in two phase: In the first, balance and exchange with calcite was considered and, in a second phase, arsenic adsorption onto the surface of iron hydroxide was modeled. The reactions with the following surfaces were employed:

Surface species:

$$\text{Surf OH} = \text{Surf OH} \quad \log K\ 0.0$$

$$\text{Surf OH} + \text{H}^+ = \text{Surf OH}_2^+ \quad \log K\ 7.29$$

$$\text{Surf OH} = \text{Surf O}^- + \text{H}^+ \quad \log K - 8.93$$

$$\text{Surf OH} + \text{AsO}_4^{3-} + 3\text{H}^+ = \text{Surf H}_2\text{AsO}_4 + \text{H}_2\text{O} \quad \log K\ 29.31$$

$$\text{Surf OH} + \text{AsO}_4^{3-} + 2\text{H}^+ = \text{Surf HAsO}_4^- + \text{H}_2\text{O} \quad \log K\ 23.51$$

$$\text{Surf OH} + \text{AsO}_4^{3-} = \text{Surf OHAsO}_4^{3-} \quad \log K\ 10.58$$

Solution species:

$$\text{H}_3\text{AsO}_4 = \text{AsO}_4^{3-} + 3\text{H}^+ \quad \log K - 20.7$$

$$\text{H}^+ + \text{AsO}_4^{3-} = \text{HAsO}_4^{2-} \quad \log K\ 11.50$$

$$2\text{H}^+ + \text{AsO}_4^{3-} = \text{H}_2\text{AsO}_4^- \quad \log K\ 18.46$$

Table 7 shows that arsenic concentration decreases at a high rate as equilibrium and ion exchange reactions with

the calcite occurs; on the other hand, arsenic concentration continues decreasing at a slower rate as adsorption occurs onto iron oxyhydroxides. Therefore, calcite showed a greater arsenic retention capacity than iron oxyhydroxides because arsenic retention onto iron oxyhydroxides surfaces was least active.

Conclusions

The urgent demand for water to meet the needs of residents in the Huautla mining district resulted in exploitation of the nearest groundwater. This groundwater was obtained from the mines in the area, which flooded from a rise in the groundwater level after they were abandoned.

This article presents the preliminary results of a study carried out in this area related to the pollution of surface water and groundwater. This research is the first work of this nature to have been conducted in the area, and therefore, the results and conclusions are a first approach to this problem.

Groundwater in the district usually is slightly saline. High contents of As, Fe, Mn, Cd, and Pb were found in groundwater in concentrations higher than the limits set by the WHO guidelines and Mexican standards for drinking water. The presence of these elements was related to sulfide mineralization.

The positive correlation between As with Fe and sulfate makes it reasonable to consider oxidation of sulfides as the source of arsenic. Considering pH and *Eh* conditions and the dissolved ions in the water, a likely mechanisms would be adsorption of arsenate onto iron oxyhydroxides surfaces, competitive adsorption among anions or adsorption on precipitated carbonates. More detailed studies could test the feasibility of this desorption.

Acknowledgments This research was supported by Consejo Nacional de Ciencia y Tecnología de México (CONACYT, Project No. 47076). We appreciate comments by the anonymous reviewers, which helped to improve the manuscript.

References

Antunes IMHR, Albuquerque MTD (2013) Using indicator kriging for the evaluation of arsenic potential contamination in an abandoned mining area (Portugal). Sci Total Environ 442:545–552. doi:10.1016/j.scitotenv.2012.10.010

APHA, Awwa, WEF (2005) Standard methods for the examination of water and wastewater, 21st edn. APHA, AWWA, WEF, Washington, DC, p 1236

Appelo CAJ, Postma D (2005) Geochemistry, groundwater and pollution, 2nd edn. Balkema, Rotterdam, p 649

Armienta MA, Segovia N (2008) Arsenic and fluoride in the groundwater of Mexico. Environ Geochem Health 30:345–353. doi:10.1007/s10635-008-9167-8

Armienta MA, Villaseñor G, Rodriguez R, Ongley LK, Mango H (2001) The role of arsenic bearing rocks in the groundwater pollution at Zimapan Valley, Mexico. Environ Geol 4–5:571–581

Avilés M, Garrido SE, Esteller MV, De La Paz JS, Najera C, Cortés J (2013) Removal of groundwater arsenic using a household filter with iron spikes and stainless steel. J Environ Manag 131:103–109. doi:10.1016/j.jenvman.2013.09.037

Bhattacharya P, Jacks G, Ahmed KM, Routh J, Khan AA (2002) Arsenic in groundwater of the Bengal Delta Plain aquifers in Bangladesh. Bull Environ Contam Toxicol 69:538–545

Biswas A, Gustafsson JP, Neidhardt H, Halder D, Kundu AK, Chatterjee D, Berner Z, Bhattacharya P (2014) Role of competing ions in the mobilization of arsenic in groundwater of Bengal Basin: insight from surface complexation modeling. Water Res 55(15):30–39. doi:10.1016/j.watres.2014.02.00

Boulding JR, Ginn JS (2004) Practical handbook of soil, vadose zone, and ground-water contamination. Assessment, prevention, and remediation, 2nd edn. Lewis Pub, Boca Raton, p 691

Bundschuh J, Litter MI, Bhattacharya P (2012) Arsenic in Latin America, an unrevealed continent: occurrence, health effects and mitigation. Sci Total Environ 429:1–332. doi:10.1016/j.scitotenv.2012.04.047 (Special issue)

Buragohain M, Bhuyan B, Sarma HP (2010) Seasonal variation of lead, arsenic, cadmium and aluminium contamination of groundwater in Dhemaji district, Assam, India. Environ Monit Assess 170:345–351. doi:10.1007/s10661-009-1237-6

Carrillo A, Drever JI (1998) Adsorption of arsenic by natural aquifer material in the San Antonio-El Triunfoo mining area, Baja California, Mexico. Environ Geol 35(4):251–257

Carrillo-Chávez A, Drever JJ, Martínez M (2000) Arsenic content and groundwater geochemistry of San Antonio-El Triunfo, Carrizal and Los Planes aquifers in southernmost Baja California, Mexico. Environ Geol 39(11):1295–1303

Castro-Larragoitia J, Kramar U, Monroy-Fernández MG, Viera-Décida F, García-González EG (2013) Heavy metal and arsenic dispersion in a copper-skarn mining district in a Mexican semi-arid environment: sources, pathways and fate. Environ Earth Sci 69:1915–1929. doi:10.1007/s12665-012-2024-1

Chakraborti D, Rahman MM, Murrill M, Das R, Patil SSG, Sarkar A, Dadapeer HJ, Yendigeri S, Ahmed R, Das KK (2013) Environmental arsenic contamination and its health effects in a historic gold mining area of the Mangalur greenstone belt of Northeastern Karnataka, India. J Hazard Mater 262:1048–1055

DOF Diario Oficial de la Federación (2000) Modificación a la Norma Oficial Mexicana NOM 127-SSA1-1994. Salud Ambiental. Agua para uso y consumo humano. Límites permisibles de calidad y tratamientos a que debe someterse el agua para su potabilización. Secretaria de Salud. México. Diario Oficial de la Federación, 22 de noviembre de 2000

DOF Diario Oficial de la Federación (2005) Norma Oficial Mexicana. Salud Ambiental NOM 230-SSA1-2002. Agua para uso y consumo humano. Requisitos sanitarios que se deben cumplir en los sistemas de abastecimiento públicos y privados durante el manejo del agua. Procedimientos sanitarios para el muestreo. Secretaria de Salud. México. Diario Oficial de la Federación, 15 de julio de 2005

Flakova R, Zenisova Z, Sracek O, Krcmar D, Ondrejkova I, Chovan M, Lalinská B, Fendekova M (2012) The behavior of arsenic and antimony at Pezinok mining site, southwestern part of the Slovak Republic. Environ Earth Sci 66(4):1043–1057. doi:10.1007/s12665-011-1310-7

Gao X, Wang Y, Hy Q, Su C (2011) Effects of anion competitive adsorption on arsenic enrichment in groundwater. J Environ Sci Health Part A 46:471–479. doi:10.1080/10934529.2011.551726

Gemici Ü (2008) Evaluation of the water quality related to the acid mine drainage of an abandoned mercury mine (Alaşehir, Turkey). Environ Monit Assess 147:93–106. doi:10.1007/s10661-007-0101-9

Gutiérrez-Ojeda C (2009) Determining the origin of arsenic in the Lagunera region aquifer, Mexico using geochemical modeling. In: Bundschuh J, Armienta MA, Biskle P, Bhattacharya P, Matschullat J, Mukherjee AB (eds) Natural arsenic in groundwater of Latin America. CRC Press, Boca Raton, pp 163–170

Iskandar I, Koike K (2011) Distinguishing potential sources of arsenic release to groundwater around a fault zone containing a mine site. Environ Earth Sci 63:595–608. doi:10.1007/s12665-010-0727-8

Lee JY, Choi JC, Yi MJ, Kim JW, Cheon JY, Choi YK, Choi MJ, Lee KK (2005) Potential groundwater contamination with toxic metals in around an abandoned Zn mine, Korea. Water Air Soil Pollut 165:167–185

Martínez-Villegas N, Briones-Gallardo R, Ramos-Leal JA, Avalos-Borja M, Castañón-Sandoval AD, Razo-Flores E, Villalobos M (2013) Arsenic mobility controlled by solid calcium arsenates: a case study in Mexico showcasing a potentially widespread environmental problem. Environ Pollut 176:114–122. doi:10.1016/j.envpol.2012.12.025

Parkhurst DL Appelo CAJ (1999). User's guide to PHREEQC (version 2)—a computer program for speciation, reaction-path, 1D-transport, and inverse geochemical calculations. US Geol Surv Water Resour Inv Rep 99-4259, p 312

Ramos OE, Rötting TS, French M, Sracek O, Bundschuh J, Quintanilla J, Bhattacharya P (2014) Geochemical processes controlling mobilization of arsenic and trace elements in shallow aquifers and surface waters in the Antequera and Poopó mining regions. Bolivian Altiplano. J Hydrol 518(Part C):421–433. doi:10.1007/s12665-011-1288-1

Rodriguez R, Ramos JA, Armienta MA (2004) Groundwater arsenic variations: the role of local geology and rainfall. Appl Geochem 19(2):245–250. doi:10.1016/j.apgeochem.2003.09.010

Rodríguez-Licea F, Sánchez-Montes de Oca R, Gamboa-Avitia A (1962) Estudio geológico – minero del Distrito de Huautla, Morelos. Archivo Técnico del Consejo de Recursos Minerales. Servicio Geológico Mexicano, México

Schulze JG (1959) Contribución al estudio petrológico y mineralógico económico del mineral de Huautla, Morelos. Archivo Técnico del Consejo de Recursos Minerales. Servicio Geológico Mexicano, México

SECOFI Secretaría de Comercio y Fomento Industrial (1998) Informe de la carta geológica-minera y geoquímica. Hoja de Cuernavaca E14-5. Secretaría de Comercio y Fomento Industrial. Consejo de Recursos Minerales- Coordinación General de Minería. Chilpancingo, México

SGM Servicio Geológico Minero (2008) Monografía geológico-minera del Estado de Morelos. Servicio Geológico Minero. Secretaría de Economía. Gobierno Federal, México

Smedley PL, Kinniburgh DG (2002) A review of the source, behaviour and distribution of arsenic in natural waters. Appl Geochem 17:517–568. doi:10.1016/S0883-2927(02)00018-5

Sracek O, Bhattacharya P, Jacks G, Gustafsson JP, Von Brömssen M (2004) Behavior of arsenic and geochemical modeling of arsenic enrichment in aqueous environments. Appl Geochem 19:169–180. doi:10.1016/j.apgeochem.2003.09.005

Vivona R, Preziosi E, Madé B, Giuliano G (2007) Occurrence of minor toxic elements in volcanic-sedimentary aquifers: a case study in central Italy. Hydrogeol J 15:1183–1196. doi:10.1007/s10040-007-0169-x

Waterloo Hydrogeologic Inc (1999) User's manual. AquaChem (v 3.7)

WHO World Health Organization (2006) Guidelines for drinking water quality. World Health Organization, Genève

Wilkie JE, Heering JG (1996) Adsorption of arsenic onto hydrous ferric oxide: effects of adsorbate/adsorbent rations and co-occurring solutes. Colloids Surf A 107(20):97–110

Winkela LHE, Casentinia B, Bardellid F, Voegelina A, Nikolaidisd NP, Charlete L (2013) Speciation of arsenic in Greek travertines: co-precipitation of arsenate with calcite. Geochim Cosmochim Acta 106(1):99–110. doi:10.1016/j.gca.2012.11.049

Wurl J, Mendez-Rodriguez L, Acosta-Vargas B (2014) Arsenic content in groundwater from the southern part of the San Antonio-El Triunfo mining district, Baja California Sur, Mexico. J Hydrol 518:447–459. doi:10.1016/j.jhydrol.2014.05.009